

# PARAMETER SWEEP STRATEGIES FOR SENSING USING BIFURCATIONS IN MEMS

C.B. Burgner<sup>1\*</sup>, K.L. Turner<sup>1</sup>, N.J. Miller<sup>2</sup>, and S.W. Shaw<sup>2</sup>

<sup>1</sup>University of California-Santa Barbara, Santa Barbara, California, USA

<sup>2</sup>Michigan State University, East Lansing, Michigan, USA

## ABSTRACT

In this work we consider a sensing strategy using dynamic bifurcations in MEMS resonators. We examine the statistics of jump events that occur as a result of a linear parameter sweep through a subcritical pitchfork bifurcation in a parametrically driven MEMS resonator in the presence of noise. The statistics of jump events are compared to those derived from a simple one-dimensional model and are found to have good agreement. Issues related to how system and input parameters affect these statistics are described, and sweeping strategies that lead to precise, fast estimates of the bifurcation point, as essential for these sensors, are derived. It is shown that for a typical MEMS resonator an optimal sweep rate exists, and noise may need to be added to achieve optimal sensitivity.

## INTRODUCTION

Nonlinear systems often exhibit jump events near bifurcation points. Common examples include the jump events encountered in the frequency response of nonlinear MEMS resonators; see, for example, Figure 1 (top). These jump events result in sudden and significant changes in response and thus may be exploited for highly sensitive measurements. Examples include threshold and linear amplification modes of the Josephson bifurcation amplifier [1], parametric measurements of a NEMS Duffing resonator [2], and frequency estimation of a parametrically forced MEMS resonator [3]. It has been proposed that such measurement methods be employed for mass sensing [4]. Noise in MEMS result in a smearing of the observed bifurcation point. Accordingly, we examine the statistics of jump events as a result of linear parameter sweeps.

In this paper we concern ourselves with the jump events that occur during a sweep through the subcritical pitchfork bifurcation in a parametrically resonant MEMS device. The frequencies at which the jumps occur are not fixed. Indeed they depend on the parameter sweep rate, and even for a fixed sweep rate they are randomly distributed as a result of thermal noise. As an example, distributions of jump events for a particular device for sweep rates spanning 0.004-0.4Hz/sec at ambient noise are shown in Figure 2. The device is the parametrically driven gyroscope described in [5]. For this resonator, which has linear natural frequency 8.4888kHz, the jump events vary by up to 3Hz, depending on sweep rate. In addition, jumps generally occur after the bifurcation point, which is estimated to be at 8.4851kHz according to the measured parameters of our model. The width of the distributions ranges from approximately 0.1Hz to 0.5Hz for individual sweep rates, see Figure 2. The aim of this work is to examine the distributions of these jump events and compare them to the predictions from a one-dimensional, single parameter model, and to use the results to derive optimal sweeping strategies. Results such as these are required for one to effectively exploit dynamic bifurcations for sensing in MEMS.

## THEORY

Near simple bifurcation points, such as the pitchfork considered here, there is a slowing down of the system dynamics in the phase space along the direction of the critical eigenvalue, and a

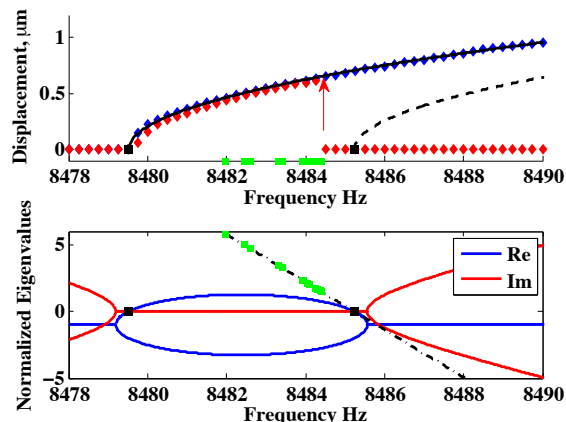


Figure 1: Nonlinear frequency response (top) showing sweeps up (blue) and down (red), compared to predicted frequency response (black), for the device shown in Figure 4. The jump events of interest are indicated. Eigenvalues of the fixed point at zero (bottom), real (blue) and imaginary (red) parts. Black dashed line illustrates the linear sweep approximation. Dots (green) show mean values of measured escape events from Figure 5.

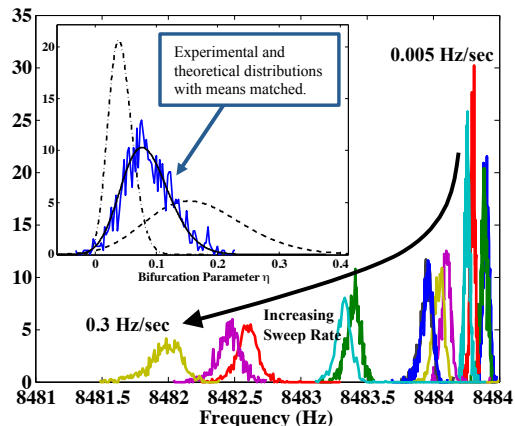


Figure 2: Distributions of jump events for a variety of sweep rates at ambient noise. Jump events result from thermal and electrical noise with effective temperature  $T=388.7^\circ\text{K}$ . Inset shows three distributions for  $\alpha=0.041$  along with mean-value-shifted measured distribution, as described in the text.

collapse onto an attendant one-dimensional manifold. When noise is present, the reduction onto the slow manifold must simultaneously treat the deterministic and stochastic aspects of the system [6]. We assume the noise to be additive, Gaussian, and white. For the subcritical pitchfork bifurcation the nondimensional stochastic normal form is given by

$$\dot{x} = 2\eta x + 4x^3 + \sqrt{D}\xi(t), \quad (1)$$

where  $x$  is the dynamic state on the slow manifold,  $\eta$  is the

bifurcation parameter (proportional to the slow eigenvalue) taken to be zero at the bifurcation point,  $D$  is the effective noise strength, and  $\xi$  is a Gaussian white noise process with zero mean and covariance equal to 2. The system can be thought of as a particle in a time-varying potential, as illustrated in Figure 3, subject to a random force. As the system is swept through the bifurcation point,  $\eta$  changes from negative to positive, resulting in the change of the effective potential as shown in Figure 3, and a loss of local stability at  $x=0$ . To create a simple linear sweep model, we approximate this change with a first order expansion of  $\eta$  in time. Thus, we assume

$$\eta = \eta_0 + rt, \quad \eta_0 < 0, \quad \text{and} \quad r > 0, \quad (2)$$

where  $r$  is the effective sweep rate and is proportional to the lab frame sweep rate (e.g., the time rate of change of the forcing frequency). The linear approximation of the bifurcation parameter corresponds to a linear approximation of the slow eigenvalue, shown in Figure 1 (bottom). This approximation is valid as long as escape occurs close to the bifurcation. Since  $\eta$  is linearly related to time, we replace time in equation (1) with bifurcation parameter and scale according to

$$\eta = r^{1/2}\tau, \quad x = r^{1/4}y. \quad (3)$$

This yields the one-parameter normal form,

$$\frac{\partial y}{\partial \tau} = 2\tau y + 4y^3 + \sqrt{\alpha}\xi(\tau), \quad (4)$$

$$\alpha = D/r. \quad (5)$$

Equation (4) universally captures the dynamics near a subcritical pitchfork bifurcation during a parameter sweep, and thus the model is not device dependent, but is broadly applicable in the manner of a normal form. Equation (4) allows one to solve for a one-parameter family of normalized escape distributions. These normalized distributions describe the probability density of a jump event occurring at a specific  $\tau$ . The single parameter,  $\alpha$ , is the ratio of noise strength to sweep rate.

As stated above, the model employed in this work is local to the vicinity of the bifurcation point. Accordingly, we define a jump event to have occurred when  $y$  escapes to  $\pm\infty$ . Closed form approximate solutions for the distribution of jump events may be found when  $\alpha$  is either very small or very large compared to unity [6]. In the interim region the problem must be solved numerically [7]. These solutions are identical for a large class of initial conditions because the system is diffusive and settles into a quasi-steady-state early in the sweep process [7,8].

The escape distributions found by solving equation (4) are functions of  $\tau$  and depend on the single parameter,  $\alpha$ . Equation (3) is used to transform these solutions into functions of the bifurcation parameter  $\eta$ , which now depend on two parameters,  $r$  and  $D$ . Thus for two sets of  $r$  and  $D$  that have identical ratio, the escape distributions, as a function of the bifurcation parameter, are related by a simple scaling. To illustrate this, the inset in Figure 2 shows three escape distributions with identical  $\alpha$  but different  $r$  and  $D$ . A corresponding experimentally measured distribution is also shown. The mean of this experimentally measured distribution is artificially shifted, for reasons discussed, to compare its shape with the theoretical curve.

Despite the discrepancy in the mean escape times predicted

by the model, it is clear that this system exhibits a distribution of escape events after the bifurcation point. Escape may, in principle, also occur before the bifurcation point. Whether it is likely to occur before or after depends on the value of  $\alpha$ . For large  $\alpha$  the sweep rate to noise is small and jump events tend to occur before the bifurcation point is reached; this is known as noise-activated escape [9-11]. For small  $\alpha$ , the sweep rate to noise is large, and jumps generally occur beyond the bifurcation; this is known as delayed bifurcation [12-14], which occurs, for example in laser turn-on dynamics. See [7] for further discussion and references.

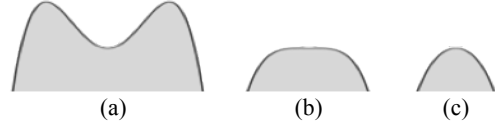


Figure 3: Illustration of the effective one-dimensional potential at three times; before (a), at (b), and after (c) the bifurcation point.

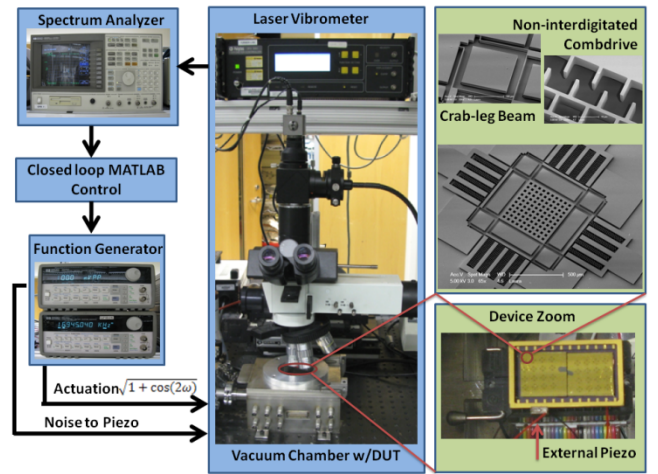


Figure 4: Experimental setup schematic with SEM of the device and close ups of the noninterdigitated combdrives and suspension.

## EXPERIMENT

The aforementioned MEMS gyroscope is fully characterized to quantitatively compare experimentally measured jump distributions with the predictions. The experimental setup is shown in Figure 4 and consists of a function generator to sweep the parametric drive frequency, a laser vibrometer to measure the device response, and a spectrum analyzer to detect bifurcation events, all controlled in MATLAB. Frequency is swept downward; if a jump event is detected, the frequency at which it occurred is noted, the input voltage is cut to allow the device time to settle back to the noise floor, and the frequency is returned to a value well above the bifurcation point before the procedure is repeated. The actuation voltage was determined to be 15Volts to allow for a wide frequency window in which escape might occur. The widest range of frequency sweep rates allowable by the lab equipment was conducted. The range of sweep rates, 0.004-0.4Hz/sec, is limited by the interplay of the characteristic response time of the device, delay in communication between hardware components, and the resolution of the frequency generator. The device is placed in vacuum and maintained at 1mTorr, resulting in a quality factor of near 3000.

In order to explore a wide range of sweep rate to noise ratios ( $\alpha$  values), a piezo-element is mounted next to the device and white noise is injected into the system, inducing random base

excitation. Both the ambient and piezo-enhanced noise are characterized by fitting a Lorentzian to the resonant peak, which rises above the laser vibrometer noise floor. The ambient noise is found to have an effective temperature of 388.7°K.

While the device used in this work exhibits two resonant modes [5], the drive and sense modes are mismatched by over 7%. This mismatch permits us to ignore the sense mode and model the drive mode as a 1DOF mass spring damper system with position dependent forcing from the non-interdigitated combdrives and cubic stiffness from the crab-leg suspension. The reduced 1DOF system dynamics is governed a nonlinear Mathieu equation and has been studied extensively [15,16],

$$\ddot{z} + Q^{-1}\dot{z} + z + \lambda(1 + \cos \Omega t)z + \gamma z^3 = \sqrt{\frac{k_B T}{mQ\omega_0^2}} \xi(t) \quad (6)$$

where  $z$  is the position,  $\omega_0$  is the natural frequency,  $\Omega$  is the normalized forcing frequency,  $Q$  is the quality factor,  $\lambda$  is the parametric forcing parameter,  $\gamma$  is the nonlinear stiffness coefficient,  $k_B$  is Boltzmann's constant,  $T$  is temperature,  $m$  is the resonator mass, and  $\xi$  is a white noise force. The device parameters were determined by fitting the experimental measured power spectral densities, measured for  $\lambda=0$  (not shown), and parametric resonance response (Figure 1).

In order to have good statistical confidence, thousands of jump events were recorded for several sweep rates and noise levels. The resonant frequency is recorded at the beginning of each test to correlate the mean of each distribution, thus accounting for the effects of drift. The drift observed was noted to be periodic, and correlated to the HVAC cycles of the lab environment.

## DISCUSSION

The frequency distributions are shown to be in good qualitative agreement with theory; see Figures 5 and 6. As expected from theory, faster sweep rates result in wider jump distributions and a shift in the mean value further past the bifurcation frequency. Figures 5 and 6 show data and theoretical curves (from equation (4)) for the normalized values of escape mean and variance respectively. The data points appearing inside the box with heading ‘gyro’ correspond to experiments done under ambient noise. The remaining data points correspond to experiments in which artificial noise was added. The boxes with headings ‘Manalis’ and ‘Roukes’ illustrate the estimated ranges of the sweep to noise ratio we expect from devices studied by Manalis [17] and Roukes [18], were they to be operated under thermal noise in a manner similar to the gyro. This illustrates how the effect of thermal noise depends on device size, as the Manalis device is 140, and the Roukes device is 242, times smaller (by mass) than the gyro. The strength of thermal noise was estimated according to the fluctuation-dissipation theorem. Thus the quality factors of these devices come into play as well. They are 15000 and 1200 for the Manalis and Roukes devices, respectively. It is interesting to note that even with the smallest device, thermal noise is still hardly sufficient to result in noise-activated escape before the bifurcation.

Both the mean and variance are underestimated by the theory, as seen in Figures 5 and 6. We suspect that this is because the escape events are occurring sufficiently far past the bifurcation point that the first order series expansion approximation of  $\eta$  breaks down. In Figure 1 green dots illustrate the mean values of escape frequencies (under ambient noise) and in Figure 1 (bottom) the black line illustrates the linear approximation. It is clear that the unstable eigenvalue is not linear in frequency over the range of

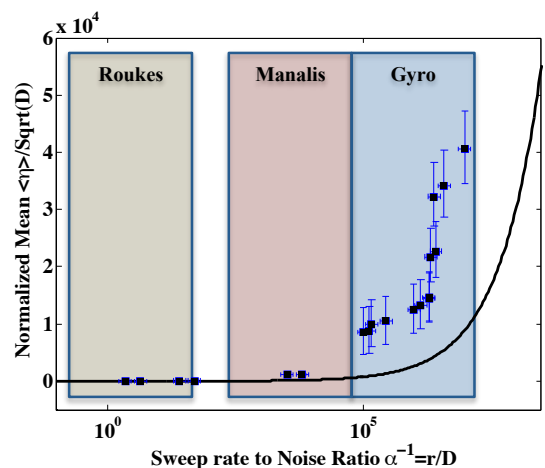


Figure 5: Normalized mean of jump frequency distributions plotted against the theoretical curve.

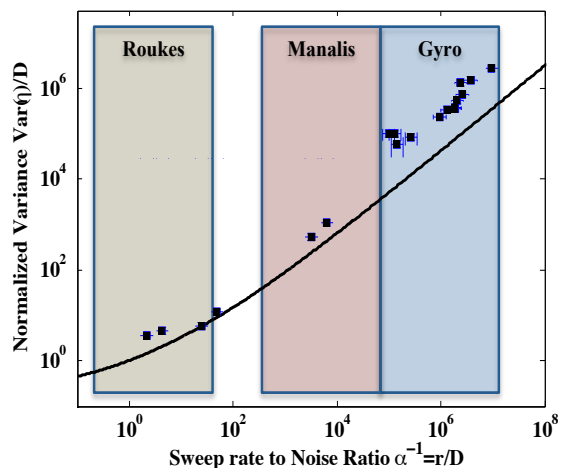


Figure 6: Normalized variance of frequency jump events plotted against theoretical curve. Slope of theoretical curve is about 1.

escape events. Accordingly, the hill shaped potential after the bifurcation point, Figure 3c, is not as sharp as our model predicts. This means that it takes more time for the system ‘particle’ to roll down the hill, and thus escape occurs later than predicted. It is because of this underestimation in the mean that we shifted the measured distribution displayed in the inset of Figure 2 in order to compare it with theory. The variance, and even the skewness (not shown), of this data matches the prediction very well. A modified theory that more accurately describes the variation of the eigenvalue may yield improved results.

One interesting application of these results is the determination of the sweep rate for a given noise level that provides the best estimate the bifurcation point within some confidence interval. Such a result is applicable when considering bifurcation point tracking as a means of mass sensing [4]. We choose a confidence interval about an estimated bifurcation point in which the real bifurcation point should exist with 90% probability. This calculation was done using the linear sweep 1D model and assuming a finite number of measurements is the only source of uncertainty. The estimated bifurcation point is found from the measured mean and variance of escape events, and using the theoretical result curves shown in Figures 5 and 6. The normalized confidence interval is shown in Figure 7. Here reset

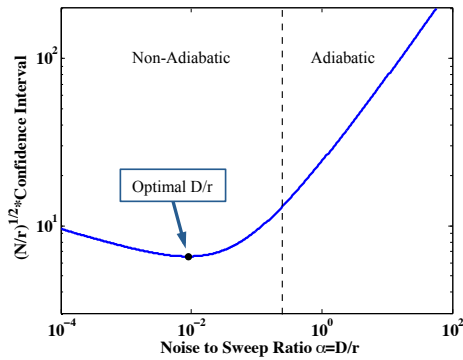


Figure 7: For a given noise level, sweep rate parameter  $r$  can be chosen to minimize the confidence interval or maximize sensitivity.

time was ignored and it was assumed that the number of escape events is  $N=crT$ , where  $c$  is some constant,  $r$  is the sweep rate, and  $T$  is the measurement time. Thus, we can use this result to determine the optimal sweep rate, given a fixed measurement time. The optimal normalized sweep rate turns out to be in the non-adiabatic region (small  $\alpha$ ), resulting in delayed bifurcations. However, since thermal noise is relatively small in MEMS devices, this rate may correspond to a relatively slow sweep in the lab frame. In order to increase measurement speed the optimal value of  $\alpha$  could be achieved by increasing noise, rather than decreasing sweep rate. This suggests that adding noise might aid in rapidly locating bifurcation points, an interesting and counterintuitive result since noise typically broadens distributions and decreases sensitivity. In this case, however, it is seen from Figure 6 that the variance of escape distributions is not increased by adding noise, at least not until a great deal of noise has been added.

## CONCLUSION

A 1D model for escape as a result of a linear parameter sweep through a pitchfork bifurcation was used to model escape events encountered in a noisy MEMS parametric resonator. The MEMS device was tested over a wide range of sweep rates and noise levels. Qualitative trends from measured data were found to be in good agreement with those predicted by theory, and variances matched quantitatively. These results illustrate the processes involved in a stochastic-dynamic bifurcations and point out the key noise to sweep rate relationship that must be understood to use this phenomenon for sensing. The model is generic and can be applied to a wide range of systems. By using the developed theory and investigating the role between noise and sweep rate, it is shown that an optimal sweep rate exists for reducing the confidence interval on the location of a bifurcation point, which can then be directly applied to determining sensitivity values in bifurcation detection schemes. Moreover, it is shown that for MEMS devices with small effective thermal noise, adding additional noise may decrease measurement time, or conversely, increase sensitivity.

## ACKNOWLEDGEMENTS

This work was supported by NSF Sensors and Sensor Systems Program Grants [0758419](#) and [0800753](#). The authors would like to thank Prof. Mark Dykman for his invaluable assistance and Dr. Laura Oropeza for device fabrication.

## REFERENCES

[1] R. Vijay, M.H. Devoret, and I. Siddiqi, "Invited Review Article: The Josephson bifurcation amplifier," *Rev. of Sci. Inst.*, Vol. 80, 111101, 2009.

[2] J.S. Aldridge and A.N. Cleland, "Noise-Enabled Precision Measurements of a Duffing Nanomechanical Resonator," *Phys. Rev. Lett.*, Vol. 94, 156403, 2005.

[3] M.V. Requa and K.L. Turner, "Precise frequency estimation in a microelectromechanical parametric resonator," *App. Phys. Lett.*, Vol. 90, 173508, 2007.

[4] W. Zhang and K.L. Turner, "Applications of parametric resonance amplification in a single-crystal silicon micro-oscillator based mass sensor," *Sensors and Actuators A*, Vol. 122(1), 23-30, 2005.

[5] L.A. Oropeza-Ramos, C.B. Burgner, and K.L. Turner, "Robust micro-rate sensor actuated by parametric resonance," *Sensors and Actuators A: Physical*, Vol. 152(1), 80-87, 2009.

[6] E. Knobloch and K.A. Wiesenfeld, "Bifurcations in Fluctuating Systems: The Center-Manifold Approach," *J. of Stat. Phys.*, Vol. 33(3), 1983.

[7] S. Shaw, N. Miller, M. Dykman, K. Turner, and C. Burgner, "Fast estimation of bifurcation conditions using noisy response data," *Proceedings of the SPIE smart structures conference*, San Diego, CA, March 2010.

[8] M.I. Dykman, B. Golding, and D. Ryvkine, "Critical Exponent Crossovers in Escape near a Bifurcation Point," *Phys. Rev. Lett.*, Vol. 92(8), 080602, 2004.

[9] M.H. Devoret, D. Esteve, J.M. Martinis, A. Cleland, and J. Clarke, "Resonant activation of a Brownian particle out of a potential well: Microwave-enhanced escape from the zero-voltage state of a Josephson Junction," *Phys. Rev. B*, Vol. 36(1), 1987.

[10] W. Wersndorfer, E. Bonet Orozco, K. Hasselbach, A. Benoit, B. Barbara, N. Demoncey, A. Loiseau, H. Pascard, and D. Mailly, "Experimental Evidence of the Neel-Brown Model of Magnetization Reversal," *Phys. Rev. Lett.*, Vol. 78(9), 1997.

[11] M. Evstigneev, "Statistics of Forced Thermally Activated Escape Events out of a Metastable State: Most Probable Escape Force and Escape-Force Moments," *Phys. Rev. E*, Vol. 78(1), 011118, 2008.

[12] P. Mandel and T. Erneux, "The Slow Passage through a Steady Bifurcation: Delay and Memory Effects," *J. of Stat. Phys.*, Vol. 48(5/6), 1987.

[13] N.G. Stocks, R. Mannella, and P.V.E. McClintock, "Influence of random fluctuations on delayed bifurcations: The case of additive white noise," *Phys. Rev. A*, Vol. 40(9), pg. 5361-5369, 1989.

[14] K.M. Jansons and G.D. Lythe, "Stochastic Calculus: Application to Dynamic Bifurcations and Threshold Crossings," *J. of Stat. Phys.*, Vol. 90(1/2), 1998.

[15] J. F. Rhoads, S. W. Shaw, K.L. Turner, J. Moehlis, B. E. DeMartini and W. Zhang, "Generalized parametric resonance in electrostatically actuated microelectromechanical oscillators," *Sound and Vibration*, 296, 797, 2006.

[16] M.I. Dykman, C.M. Maloney, V.N. Smelyanskiy, and M. Silverstein, "Fluctuational phase-flip transitions in parametrically driven oscillators," *Phys. Rev. E*, Vol. 57(5), 1998.

[17] T.P. Burg, M. Godin, S.M. Knudsen, W. Shen, G. Carlson, J.S. Foster, K. Babcock, and S.R. Manalis, "Weighing of Biomolecules, Single Cells, and Single Nanoparticles in Fluid," *Nature*, Vol. 446, pg.1066, 2007.

[18] He, R.R., Feng, X.L., Roukes, M.L., & Yang, P.D, "Self-transducing silicon nanowire electromechanical systems at room temperature," *Nano Letters* 8, 1756-1761 (2008)..

## CONTACT

\*C.B. Burgner, tel: +1-714-313-1867; [cburgner@engr.ucsb.com](mailto:cburgner@engr.ucsb.com)